Extrapolation of Proton Electromagnetic Form Factor. II*

J. S. LEVINGER† AND C. P. WANG‡
Cornell University, Ithaca, New York
(Received 30 June 1964)

We extrapolate the proton form factors to time-like momentum transfers to determine the spectral functions. We compare our extrapolations with preliminary measurements of the cross section for proton-antiproton annihilation into an electron-positron pair, for a time-like momentum transfer of 172 F^{-2}. This comparison determines an otherwise arbitrary parameter used in our conformal-transformation procedure of extrapolation. We also apply the constraint that electric and magnetic form factors are equal at time-like momentum transfer of $4M^2$. We find spectral functions with a peak around 625 MeV, a zero around 1050 MeV, and a minimum around 1500 MeV.

I. INTRODUCTION

In a previous paper[1] one of us (JSL) and R. F. Peierls used a conformal transformation[2] to facilitate extrapolation of electromagnetic form factors in the t plane from negative momentum transfers t, reached by electron-proton scattering, to positive, or time-like values of t. The purpose of this extrapolation is to determine the spectral function, which is the imaginary part of the extrapolated form factor just above the cut. We give below the notation[1] of I; the reader is referred to I for lengthy discussions of this extrapolation procedure and tests of its validity using artificial data.

A form factor $G(t)$ is related to the spectral function $g(t)$ using a subtracted dispersion relation:

$$G(t)=\frac{1}{\pi}\int_{t_0}^{\infty}\frac{g(t')dt'}{t'-t}+G(-\infty). \tag{1}$$

For the proton form factor, the spectral function starts at the threshold $t_0=4$ squared pion masses, or 2.0 F^{-2}. We solve integral Eq. (1) for the spectral function by making a conformal transformation to a new variable η:

$$\eta=[b-(1-t/t_0)^{1/2}]/[b+(1-t/t_0)^{1/2}]. \tag{2}$$

Here $b\geq 1$, but is otherwise arbitrary. In I we give reasons for choosing $b=2$, and we shall make the same choice in this paper. In Sec. IV we return to the question of how to choose the value of b, and how sensitive the determination of the spectral function is to the choice of b.

Equation (2) transforms the cut t plane into the interior of the unit circle in the η plane. We fit the measured form factors with a truncated power series in η, and determine the coefficients a_n

$$K(\eta)=\sum_{n=0}^{N}a_n\eta^n. \tag{3}$$

The order N of the polynomial is determined by statistical criteria, namely, we examine the goodness of fit χ^2 for different values of N. In general, χ^2 decreases rapidly as we increase N up to a certain value, at which point it levels off somewhere near the number of degrees of freedom.

The spectral function $g(t)$ is determined by finding the imaginary part of $K(\eta)$ at the cut in the η plane, namely,

$$g(t)=\sum_{n=1}^{N}a_n\sin n\xi(t). \tag{4}$$

Here the angle $\xi(t)$ in the η plane is given by

$$\cos\xi(t)=(b^2+1-t/t_0)/(b^2-1+t/t_0). \tag{5}$$

Equation (4) shows that we are fitting the spectral function with a truncated Fourier series.

In this paper we shall always use two constraints discussed in I: (i) that the values of the form factors given by Eq. (3) for $t=0$ agree with the very accurately known static values; (ii) that the spectral function have zero slope at threshold, corresponding to the centrifugal barrier effect for 1^- states that can join to the virtual photon in electron-proton scattering. This p-wave constraint is

$$\sum_{n=0}^{N}na_n=0. \tag{6}$$

In I we sometimes imposed the restriction that the subtraction constant $G(-\infty)$ in Eq. (1) be zero, within some chosen statistical error. This restriction is imposed in our present work, and is discussed further in Sec. IV.

We have extended our previous work in several respects. First, we are now imposing the additional constraint[3] that the complex electric and magnetic form

* Work supported in part by the U. S. Office of Naval Research.
† AVCO Visiting Professor; at Rensselaer Polytechnic Institute, Troy, New York starting Fall 1964.
‡ At Catholic University of America, Washington, D. C., starting Fall 1964.
[1] J. S. Levinger and R. F. Peierls, Phys. Rev. 134, B1341 (1964), referred to as I.
[2] W. R. Frazer, Phys. Rev. 123, 2180 (1961); C. Lovelace, Nuovo Cimento 25, 730 (1962); D. Atkinson, Phys. Rev. 128, 1908 (1962); R. Theis, Cambridge Photon Conference, 1963 (unpublished); J. D. L. Zeiler, Diplomarbeit Technische Hochschule Karlsruhe (unpublished).
[3] S. Bergia and L. Brown, Proceedings of the International Conference on Nucleon Structure, Stanford, 1963 (unpublished).

factors be equal at $t=4M^2$, where M is the proton mass,

$$G_E(4M^2)=G_M(4M^2). \tag{7}$$

Second, we are using data[4] for G_E and G_M as of April 1964, while in I we used data as of February 1963. In particular, the range has been extended from -45 $F^{-2}\leq t\leq 0$ to -175 $F^{-2}\leq t\leq 0$. Also, we now pay special attention to region $t\geq 4M^2$ reached by proton-antiproton annihilation leading to creation of an electron-positron pair. Third, we have studied the dependence of our extrapolation on the value chosen for the parameter b in Eq. (2). We give several arguments justifying the choice $b=2$.

The general conclusions of this paper are in agreement with I. In particular we find magnetic and electric spectral functions each with a strong positive peak in the region of 625 MeV, going through zero around 1050 MeV, and with a minimum around 1500 MeV. The position of the peak is consistent with large contributions by the vector ρ and ω resonances located at 750 and 785 MeV, respectively. The width of the peak is about 350 MeV, but the width is not well determined by our extrapolation procedure, and is not inconsistent with the 100-MeV width of the ρ resonance.

So far we have confirmed the conclusions reached by assuming poles in the spectral function[5]; however, as remarked in I, we have reached these conclusions without having to assume from the beginning the importance of the ρ and ω resonances. One advantage of our extrapolation procedure is that we can obtain agreement with preliminary measurements of the form factors in the annihilation region, while such agreement has not been obtained by pole fits.

II. CONSTRAINT AT $t=4M^2$

Two different arguments[3] led to Eq. (7), stating that the electric and magnetic form factors are equal at $t=4M^2$. The first argument is based on the isotropy, and absence of polarization effects, for the electron-positron pair produced by annihilation of very slow antiprotons by protons. [See Eq. (13) and related discussion below.] The second argument is based on the algebraic relations

$$\begin{aligned} G_E&=F_1+(t/4M^2)F_2,\\ G_M&=F_1+F_2. \end{aligned} \tag{8}$$

If $G_E(4M^2)\neq G_M(4M^2)$ then F_1 and F_2 would be singular at $4M^2$. [In Eq. (8) we are using the normalizations $G_E(0)=F_1(0)=1$; $F_2(0)=1.793$, the anomalous proton moment in nuclear magnetons; and $G_M(0)=2.793$, the total proton moment.]

One might hope that extrapolations of the data would automatically satisfy the constraint Eq. (7), and in fact the extrapolations in I did give electric and magnetic spectral functions (constrained quartic fits) that agreed within their statistical errors. This agreement may have been accidental, since the fits for the present data do not automatically satisfy the constraint (7). The magnetic and electric spectral functions found in Sec. IV are -1.9 ± 0.1 and -0.5 ± 0.1, respectively, so the imaginary parts disagree by 10 standard errors of the difference! The real parts of -0.8 and -0.3, respectively, are also in disagreement.

We have adopted the following trick to enforce the constraint. We treat the magnetic form factor as in I, but we use Eq. (8) to find values of the Pauli form factor F_2 from the measurements of magnetic and electric form factors for negative t

$$F_2=(G_M-G_E)/(1-t/4M^2). \tag{9}$$

We then fit these values of F_2 with a power series in η and extrapolate to the cut in the η plane. We then extrapolate G_E using the extrapolations for G_M and F_2:

$$G_E=G_M-(1-t/4M^2)F_2. \tag{10}$$

Thus we have forced the extrapolated complex G_E to equal G_M at $t=4M^2$.

We see from Eq. (10) that unless F_2 vanishes sufficiently rapidly for $|t|\to\infty$, we will obtain infinite values for G_E. In this paper we insist that tF_2 remain finite, but we allow this finite value to give us a finite subtraction constant for G_E. We keep tF_2 finite by imposing two *more* constraints on the power series fit in η with coefficients c_n:

$$\sum_{n=0}^{N}(-1)^n c_n=0; \quad \sum_{n=0}^{N}(-1)^n n c_n=0. \tag{11}$$

III. EXTRAPOLATION OF CURRENT FORM FACTOR DATA

We apply the methods of the previous two sections to current data[4] (April 1964) given in Table I. Here and throughout this section we use $b=2$. Note that for the magnetic form factor we have added the assumed datum at $t=-\infty$; see the discussion in Secs. I and IV. [For F_2 the behavior at $-\infty$ is covered by the constraints (11).]

Since we need data on both electric and magnetic form factors at the same momentum transfer to find the Pauli form factor F_2, we have omitted measurements of the electric form factor for $-1<t<0$, where there are no measurements of the magnetic form factor. At momentum transfers t of -6, -10, -14, and -18 F^{-2} we have combined two or three measurements of the electric form factor. (The data were not independent, so we have only estimated rather than calcu-

[4] R. R. Wilson and J. S. Levinger, Ann. Rev. Nucl. Sci. **14** (1964).

[5] J. S. Levinger, Nuovo Cimento **26**, 813 (1962); S. Goto, *ibid.* **27**, 1249 (1963); L. N. Hand, D. G. Miller, and R. Wilson, Rev. Mod. Phys. **35**, 335 (1963); C. Akerlof, K. Berkelman, G. Rouse, and M. Tigner, Phys. Rev. **135**, B810 (1964); A. P. Balachandran, P. G. O. Freund, and C. R. Schumacher, Phys. Rev. Letters **12**, 209 (1964).

TABLE I. Data on proton electromagnetic form factors. The variable η is given by Eq. (2), with $b=2$; the datum for G_M at infinity is assumed, while the F_2 value at infinity is given by constraint (11). The error given on F_2 assumes a correlation coefficient of -1 between the statistical errors quoted for G_M and G_E.

t (F^{-2})	η	Magnetic G_M	Error	Electric G_E	Error	Pauli F_2	Error	Ref.
−1.0	0.240	2.511	0.038	0.881	0.009	1.609	0.046	a
−1.6	0.197	2.394	0.025	0.850	0.010	1.517	0.034	b
−2.0	0.172	2.234	0.034	0.784	0.012	1.419	0.045	a
−2.98	0.118	2.034	0.016	0.725	0.021	1.267	0.036	c
−4.6	0.048	1.731	0.025	0.628	0.013	1.049	0.036	d
−6.0	0.000	1.471	0.031	0.570	0.019	0.840	0.047	d, e
−7.0	−0.029	1.383	0.028	0.539	0.021	0.783	0.045	d
−7.5	−0.043	1.335	0.025	0.520	0.020	0.752	0.042	d
−8.0	−0.056	1.308	0.020	0.462	0.016	0.777	0.033	d
−9.0	−0.079	1.240	0.022	0.427	9.021	0.739	0.039	d
−10.0	−0.101	1.130	0.022	0.417	0.020	0.642	0.038	d
−11.0	−0.121	1.075	0.020	0.409	0.020	0.593	0.036	d
−12.0	−0.138	0.979	0.022	0.389	0.021	0.521	0.038	d
−13.0	−0.156	0.913	0.039	0.374	0.037	0.471	0.066	d
−14.0	−0.172	0.887	0.025	0.350	0.029	0.462	0.047	d, e
−15	−0.186	0.831	0.048	0.326	0.055	0.433	0.088	d
−16	−0.206	0.795	0.014	0.285	0.021	0.433	0.030	d
−17	−0.213	0.773	0.020	0.260	0.032	0.431	0.044	d
−18	−0.225	0.704	0.014	0.301	0.020	0.336	0.028	d, e
−19	−0.236	0.691	0.017	0.274	0.032	0.344	0.040	d
−20	−0.248	0.673	0.031	0.203	0.072	0.385	0.084	d
−22	−0.268	0.633	0.020	0.155	0.075	0.384	0.076	d
−25	−0.295	0.447	0.016	···	···	···	···	f
−30	−0.333	0.382	0.014	···	···	···	···	f
−30	−0.333	0.422	0.04	0.164	0.05	0.194	0.068	g
−35	−0.366	0.314	0.012	···	···	···	···	f
−40	−0.393	0.232	0.018	···	···	···	···	f
−45	−0.416	0.238	0.022	···	···	···	···	f
−45	−0.416	0.240	0.024	0.124	0.04	0.077	0.043	g
−75	−0.512	0.131	0.014	0.035	0.035	0.052	0.027	g
−100	−0.562	0.089	0.012	0.032	0.032	0.027	0.021	g
−125	−0.599	0.04	0.02	0.04	0.04	0.000	0.025	g
−175	−0.650	0.03	0.015	0.04	0.05	−0.003	0.022	g
$-\infty$	−1.00	0.00	0.03	···	···	0.00	0.00	

[a] B. Dudelzak, G. Sauvage, and P. Lehmann, Nuovo Cimento 28, 18 (1963).
[b] D. J. Drickey and L. N. Hand, Phys. Rev. Letters 9, 521 (1962).
[c] P. Lehmann, R. Taylor, and R. Wilson, Phys. Rev. 126, 1183 (1962).
[d] T. Janssens, R. Hofstadter, E. B. Hughes, and M. R. Yearian (to be published).
[e] J. R. Dunning, K. W. Chen, N. F. Ramsey, *et al.*, Phys. Rev. Letters 10, 500 (1963): and K. W. Chen (private communication).
[f] K. Berkelman, M. Feldman, R. M. Littauer, G. Rouse, and R. R. Wilson, Phys. Rev. 130, 2061 (1963).
[g] K. W. Chen, A. A. Cone, J. R. Dunning, Jr., *et al.*, Phys. Rev. Letters 11, 561 (1963), and (private communication).

lated the error of the averaged value.) At $t\leq -75$ F^{-2}, the data needed interpretation to give the values quoted in Table I, particularly as regards the electric form factor. For instance, at $t=-75$ F^{-2}, the experimentalists quote $G_E=0.00$ $(+0.069-0.00)$. The asymmetry of the quoted errors is due to their measurement of G_E^2, and the condition that G_E^2 must be nonnegative. We have arbitrarily reinterpreted their result as $G_E=0.035\pm0.035$; this interpretation shows our prejudice for nonnegative values of G_E. We have treated G_E at $t=-100$ F^{-2} in a similar manner. At $t=-125$ F^{-2}, only one measurement was made, so we know only that

$$0.4\,G_E^2+0.8G_M^2=0.0025\pm0.0005,$$

which we have interpreted as $G_E=0.04\pm0.04$, and $G_M=0.04\pm0.02$. For the highest momentum transfer, $t=-175$ F^{-2}, only an upper limit on the differential cross section was found, giving upper limits on G_E and G_M of 0.09 and 0.05, respectively, which we have

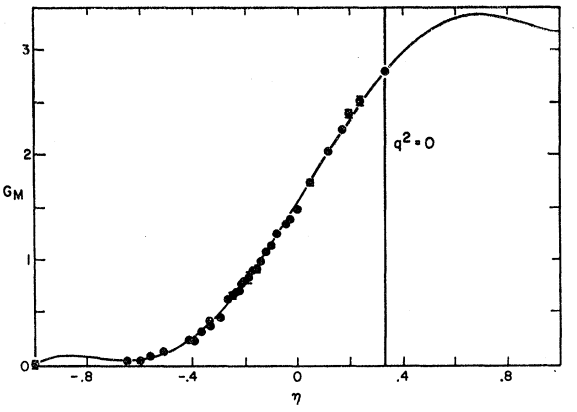

FIG. 1. The proton magnetic form factor G_M versus the variable η defined by the conformal transformation (2) for $b=2$. The points show the data of Table I; the curve shows the polynomial fit of Table IV.

interpreted with our prejudice for positive proton form factors.

The data of Table I were fitted by the procedures of Secs. I and II; also see the Appendix of I for least-squares fits with constraints. We have used two constraints in fitting the magnetic form factor [Eq. (6), and discussion above], and two additional constraints (11) in fitting the Pauli form factor F_2. The χ^2 values given in Table II for the magnetic form factor fits clearly level off at $N=5$; we therefore use a constrained quintic fit. The value 66.1 is clearly large by statistical criteria for our system with only 30 degrees of freedom; but a study of the data of Table I strongly suggests that this large χ^2 value is due to disagreements among different laboratories, e.g., the sudden drop in G_M from 0.633 ± 0.020 at $t=-22$ F^{-2} to 0.447 ± 0.016 at $t=-25$ F^{-2}. As Fig. 1 shows, the quintic fit interpolates between these data in a smooth manner. Table II gives χ^2 values for the F_2 fits that level off at $\chi^2=15.4$ for a sextic, through the χ^2 value of 35.1 for a quintic is statistically acceptable. We adopt the sextic fit.

The coefficients a_n for the quintic fit to the magnetic form factor and c_n for the sextic fits to the Pauli form factor are given in Table III. We give the diagonal errors in these coefficients, as a rough indication of the errors in the extrapolations, but the complete error

TABLE II. χ^2 values versus degree of polynomial. We use the data of Table I; the magnetic fit uses constraint (6) and the Pauli fit uses the additional constraints (11).

Degree of polynomial N	χ^2 for magnetic form factor G_M	χ^2 for Pauli form factor F_2
3	443.6	2318
4	276.7	56.0
5	66.1	35.1
6	65.0	15.4
7	64.7	13.3

TABLE III. Coefficients, and diagonal errors, for polynomial fits to the data of Table I; the χ^2 values for these fits are given in Table II.

n	Magnetic form factor a_n	Error	Pauli form factor c_n	Error
0	1.54	0.01	0.91	0.01
1	4.07	0.03	2.85	0.08
2	0.53	0.07	0.98	0.10
3	−4.59	0.22	−4.20	0.63
4	−0.48	0.04	−2.91	0.54
5	2.12	0.15	1.95	0.36
6	···	···	1.61	0.36

matrix is used as discussed in I for the calculations below of statistical errors of the extrapolations.

Table IV gives the values of the magnetic and Pauli form factors, and statistical errors, for real η found using the coefficients of Table III. We use Eq. (10) and these fits to G_M and F_2 to give the electric form factor G_E; the errors given for G_E are approximate, since we do not know the correlated errors between the a_n and c_n values.

Figure 1 shows a curve for the fit to magnetic form factors given in Table IV, as well as points showing the input data and errors of Table I. This figure illustrates the good fit to the data in the region where we have accurate measurements. The statistical error of the extrapolation grows rapidly as we leave the region where there are measurements, reaching 0.09 at $\eta=0.92$. The statistical error remains small in the region $-1<\eta<0.64$, since we have used a datum at $\eta=-1$, as shown in Table I. Figure 2 compares the fit to the electric form factors with the input data of Table I. Again the agreement is good, as shown by the good value of χ^2 for our fit to F_2. The subtraction constant for the electric form factor turns out to be −0.26, but not statistically different from zero.

Table V gives the spectral functions for the magnetic and Pauli form factors using the coefficients of Table III, as well as the statistical errors in the spectral functions. The electric spectral function is then determined from Eq. (10). Figure 3 plots the magnetic and electric spectral functions versus the mass of the intermediate state in MeV. The magnetic spectral function is determined with the small statistical error of about 0.2. There is a strong positive peak with a maximum near 625 MeV, and a full width at half-maximum Γ of 380 MeV. This width corresponds to a 32° width in ξ, which as discussed in I is near the minimum width expected in a Fourier series truncated at five terms. (That is, the 380-MeV width is inherent in our extrapolation procedure, and represents only an upper limit for the width of the resonance.) The values of the position of the peak and its width are virtually unchanged from the values for the restricted quintic fit to the magnetic form factors in I.

TABLE IV. Polynomial fits for real η.[a] The coefficients for the fits to the magnetic and Pauli form factors (G_M and F_2) are given in Table III; the complete error matrix is used in computing the statistical errors. The electric form factor G_E is computed from Eq. (10); its errors are approximate.

η	t (F^{-2})	G_M	Error	F_2	Error	G_E	Error
0.92	1.99	3.21	0.09	1.28	0.36	1.96	0.44
0.80	1.90	3.28	0.07	1.54	0.28	1.77	0.35
0.68	1.71	3.32	0.05	1.81	0.18	1.55	0.23
0.56	1.26	3.25	0.03	1.95	0.09	1.33	0.12
0.44	0.79	3.06	0.01	1.94	0.03	1.14	0.04
0.333	0.00	2.793	0.000	1.793	0.000	1.000	0.000
0.32	−0.12	2.753	0.001	1.768	0.003	0.985	0.004
0.20	−1.56	2.34	0.01	1.49	0.02	0.83	0.02
0.08	−3.78	1.87	0.01	1.15	0.02	0.68	0.02
−0.04	−7.38	1.38	0.01	0.80	0.01	0.51	0.02
−0.16	−13.2	0.92	0.01	0.50	0.01	0.35	0.02
−0.28	−23.3	0.54	0.01	0.27	0.01	0.20	0.02
−0.40	−41.5	0.26	0.01	0.11	0.01	0.09	0.02
−0.52	−78.1	0.10	0.01	0.03	0.01	0.04	0.03
−0.64	−180	0.05	0.01	0.01	0.01	0.03	0.04
−0.76	−427	0.07	0.01	0.006	0.010	0.04	0.07
−0.88	−1958	0.09	0.02	0.005	0.005	−0.02	0.13
−1.00	$-\infty$	−0.003	0.030	0.000	0.000	−0.26	···

[a] η is given by Eq. (2) for $b=2$.

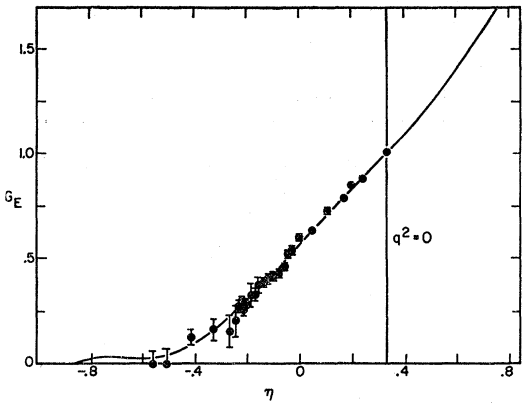

FIG. 2. The proton electric form factor G_E versus the variable η defined by Eq. (2) for $b=2$. The points show the data of Table I; the curve shows the fit of Table IV.

The magnetic spectral function goes through zero at 1050 MeV, and has a broad dip with a minimum around 1500 MeV. This dip is broad in terms of energy, but like the peak it is narrow when expressed in terms of angle ξ, namely only 26°. We also see a dip at 340 MeV, or angle ξ about 40°. From a statistical point of view this dip should be taken seriously, since it is over 6 standard errors, but since our extrapolation procedure has a tendency to produce spurious oscillations, we do not believe the 340-MeV dip is well established.

The electric spectral function, shown with statistical errors as the shaded band in Fig. 3, has the same general features as the magnetic spectral function, but has larger statistical errors. The main peak is at 750 MeV, the zero at 1170 MeV, and the minimum at 1600 MeV. (The wiggles near threshold are not of significance since the statistical errors are large.) By our method of first fitting the Pauli form factor and then determining the electric form factor, we have forced the electric spectral function to equal the magnetic spectral function at a mass of $2M$, or 1876 MeV. They remain close to each other up to 2500 MeV.

We now use our extrapolation procedure to estimate

both real and imaginary parts of the electric and magnetic form factors in the annihilation region, $t \geq 4M^2 = 90$ F^{-2}. The real and imaginary parts are then combined to give three different quantities,[6] which could be determined experimentally by measurements on electron-positron pairs or muon pairs produced by proton-antiproton annihilation. First, the total cross section for lepton pair production by this process is proportional to

$$G^2 = |G_E|^2 + (t/2M^2)|G_M|^2. \quad (12)$$

Second, the angular distribution $d\sigma/d\Omega$ in the center-of-mass system is proportional to

$$I(\theta) = 2 + A + A\cos^2\theta,$$

where

$$A = t|G_M|^2/4M^2|G_E|^2 - 1. \quad (13)$$

Finally, azimuthal effects due to annihilation of polarized antiprotons are proportional to the sine of the phase difference ϕ between the complex form factors G_E and G_M.

A preliminary measurement[7] of the total cross section at 172 F^{-2} gives $G = 2.2$, based on six electron-positron pair events. The angular distribution, and polarization effects are much more difficult to measure. In Table VI we give values for G, A, and $\sin\phi$ for t in the annihilation region. Note that by our constraint at $t = 4M^2$, we have enforced an isotropic angular distribution and no polarization effects, i.e., $A = \sin\phi = 0$. At higher values of t the anisotropy and polarization effects increase, but they are still not large at $t = 165$ F^{-2}.

This agreement with the experimental value of G represents a major advantage of our extrapolation procedure over those to date using a sum of poles.[5]

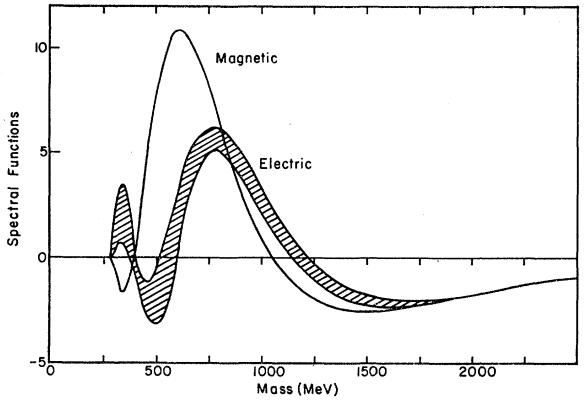

FIG. 3. The proton spectral functions for magnetic and electric form factors versus mass of the intermediate state in MeV, taken from Table V. The shaded region shows the statistical error for the electric spectral function; the statistical error for the magnetic spectral function is given in Table V.

[6] K. J. Barnes, Nuovo Cimento **28**, 284 (1963); A. Zichichi, S. M. Berman, N. Cabibbo, and R. Gatto, *ibid.* **24**, 170 (1962).
[7] M. Conversi, T. Massam, Th. Muller, and A. Zichichi, Phys. Letters **5**, 195 (1963); M. Conversi, T. Massam, Th. Muller, and A. Zichichi, *Proceedings of the Sienna International Conference on Elementary Particles, 1963*, edited by G. Bernadini and G. P. Puppi (Societá Italiana di Fisica, Bologne, 1963).

TABLE V. Spectral functions. The magnetic and Pauli spectral functions, and statistical errors, are found from the coefficients of Table III. The electric spectral function is found from Eq. (10); its errors are approximate. The mass is 197 $t^{1/2}$; the angle ξ is given by Eq. (5), with $b = 2$.

t (F^{-2})	ξ (deg)	Mass (MeV)	G_M	Error	F_2	Error	G_E	Error
2.00	0.0	280	0.00	0.00	0.00	0.00	0.00	0.00
2.12	14.9	289	−0.27	0.03	−0.67	0.16	0.38	0.19
2.42	25.8	308	−1.11	0.13	−2.69	0.67	1.51	0.78
2.90	37.3	337	−1.77	0.26	−4.05	1.12	2.15	1.34
3.56	47.5	373	−0.95	0.30	−2.14	0.92	1.11	1.18
4.46	58.1	418	1.83	0.20	2.97	0.21	−0.99	0.40
5.37	66.1	459	4.96	0.07	7.50	0.82	−2.09	0.84
6.61	74.6	509	8.21	0.18	10.72	1.39	−1.73	1.47
8.33	83.3	571	10.46	0.34	10.97	1.43	0.50	1.63
9.87	89.9	622	10.80	0.39	9.18	1.10	2.61	1.37
11.9	96.1	683	9.93	0.37	6.14	0.60	4.60	0.89
14.6	104	757	7.85	0.29	2.61	0.26	5.66	0.51
16.3	106	800	6.45	0.23	0.95	0.39	5.58	0.55
20.8	114	903	3.30	0.10	−1.59	0.66	4.52	0.60
27.4	122	1037	0.32	0.11	−2.67	0.67	2.12	0.56
32.0	126	1120	−0.87	0.14	−2.66	0.58	0.84	0.51
37.8	129	1217	−1.75	0.17	−2.37	0.45	−0.38	0.43
45.3	134	1333	−2.29	0.18	−1.90	0.31	−1.35	0.33
55.4	138	1474	−2.47	0.18	−1.34	0.17	−1.93	0.25
69.2	142	1647	−2.35	0.15	−0.82	0.08	−2.16	0.17
88.9	147	1867	−1.98	0.12	−0.39	0.07	−1.98	0.12
118	151	2154	−1.46	0.08	−0.10	0.10	−1.49	0.11
165	155	2545	−0.91	0.05	0.05	0.10	−0.87	0.13
247	160	3111	−0.41	0.03	0.10	0.07	−0.24	0.15
408	164	4000	−0.05	0.04	0.08	0.04	0.29	0.18
800	168	5600	0.14	0.04	0.04	0.02	0.43	0.20
∞	180	∞	0.00	0.00	0.00	0.00	0.00	0.00

(If the poles are confined to relatively low masses, say $t \leq 40$ F^{-2}, then the value of G predicted is quite small being of order 0.2. By construction, the imaginary parts of G_E and G_M are zero at 172 F^{-2}; and the real parts are quite small since the annihilation region is so far away from the assumed pole positions.)

IV. DISCUSSION

In this section we discuss the sensitivity of our extrapolation procedure to three different assumptions. First, we compare the spectral function for the electric form factor calculated directly from the data of Table I with that calculated in the roundabout way of Sec. II. This comparison tests the importance of the assumption

TABLE VI. Proton-antiproton annihilation into lepton pairs. t is the momentum transfer. The real parts ReG_M and ReG_E use the coefficients of Table III; ImG_M and ImG_E are the spectral functions given in Table V. The total cross section is proportional to G^2—see Eq. (12) and Refs. 4 and 6. The angular distribution is $2 + A + A\cos^2\theta$: see Eq. (13). Polarization effects are proportional to $\sin\phi$, where ϕ is the phase difference between the complex electric and magnetic form factors.

t (F^{-2})	ReG_M	Error	ReG_E	Error	G	Error	A	$\lvert\sin\phi\rvert$
89	−0.12	0.08	−0.13	0.08	3.4	0.2	0.00	0.00
118	0.41	0.09	0.55	0.13	2.9	0.2	0.36	0.08
165	0.68	0.09	0.91	0.15	2.4	0.2	0.51	0.17
247	0.71	0.07	0.94	0.10	2.1	0.2	0.96	0.27
408	0.57	0.05	0.71	0.09	1.8	0.2	1.54	0.46
800	0.35	0.03	0.32	0.13	1.6	0.2	3.30	0.52

TABLE VII. Coefficients for different polynomial fits. The restricted magnetic fit is for G_M of Table I, including the datum at infinite momentum transfer. The nonrestricted magnetic fit is for Table I, but omitting this one datum. The direct fit to the electric form factors uses G_E from Table I, with no point at infinity.

	Restricted magnetic		Nonrestricted magnetic		Direct fit to electric	
n	a_n	Error	a_n	Error	a_n	Error
0	1.544	0.007	1.545	0.007	0.563	0.005
1	4.074	0.028	4.118	0.044	1.363	0.029
2	0.529	0.073	0.558	0.076	0.124	0.078
3	−4.594	0.217	−5.066	0.425	−0.949	0.141
4	−0.482	0.038	−0.834	0.276	0.309	0.131
5	2.115	0.146	2.660	0.447	...	...
	$\chi^2=66.1$		$\chi^2=64.4$		$\chi^2=17.3$	

that $G_E(4M^2)=G_M(4M^2)$. Second, we compare the magnetic spectral function calculated both with and without the datum at infinite momentum transfer which we used in Table I. Here we test the importance of our restriction to approximately nonsubtracted dispersion relations. Finally, we examine the sensitivity of our results to the value of b used in the conformal transformation (2). We find that the calculation of G, defined in Eq. (12), is much more sensitive to the value of b than is the behavior of the spectral function near its peak.

Figure 4 shows two different calculations of the electric spectral function, both using the data of Table I, with $b=2$. The spectral function "using F_2" is from Table V and Fig. 3; the spectral function "found by direct fit" uses the coefficients given in Table VII, for a quartic fit with the low χ^2 value of 17.3 for 25 degrees of freedom. We make a nonrestricted fit and find $G_E(-\infty)=0.6\pm0.2$. Both spectral functions have their main peak near 700 MeV, but the direct quartic fit gives a much broader peak, with a width of 600 MeV. Also the direct fit gives only weak evidence for a high energy dip in the spectral function. Note the disagreement between the two curves at a mass of $2M=1876$ MeV, where the fit using F_2 is forced to have the value of the magnetic spectral function.

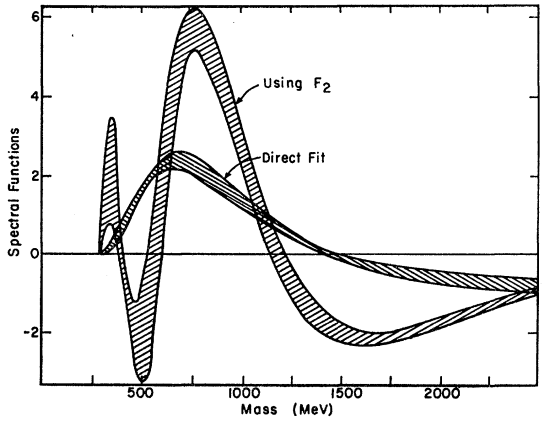

FIG. 4. Comparison of two electric spectral functions. The curve "using F_2" from Table V uses a fit to the Pauli form factor F_2. The "direct fit" is a quartic in η fitted directly to the data of Table I. The shaded regions shows the statistical errors.

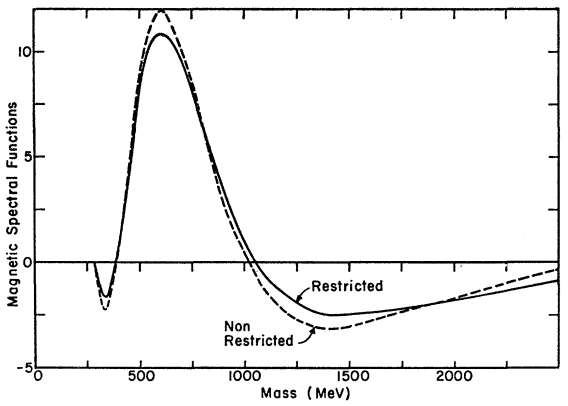

FIG. 5. Comparison of two magnetic spectral functions. The restricted quintic, taken from Table V, uses the restriction that the form factor be zero at infinite momentum transfer. The nonrestricted quintic uses the same data from Table I without the datum at infinite momentum transfer; the coefficients are given in Table VIII.

In Table VII we also compare coefficients for two different fits to the magnetic form factors of Table I. The restricted fit is that of the previous section (Table III), using the datum at infinite momentum transfer. The second, nonrestricted fit makes no assumption concerning the behavior of the magnetic form factor at infinite t. We find $G_M(-\infty)=-0.4\pm0.3$. Note that the restricted and nonrestricted fits agree closely both as to the values of N, a_n, and the χ^2 values, the main difference between them being the larger errors in a_3, a_4, and a_5 for the nonrestricted fit. Figure 5 shows that the two spectral functions found from these coefficients (solid for restricted and dashed curve for nonrestricted) agree very well. We conclude that our restriction on $G_M(-\infty)$ does not have a large effect on our extrapolation of the proton's magnetic form factor.

TABLE VIII. χ^2 values for different choices of b and N. The χ^2 values for fits to the data of Table I are given for different choices of the degree N of the polynomial, and the parameter b used in Eq. (2). In Sec. II we used $b=2$, a quintic fit for the magnetic form factor, and a sextic fit for the Pauli form factor.

	Magnetic form factor						
N	$b=1$	$b=1.5$	$b=2$	$b=2.5$	$b=3$	$b=3.5$	$b=4$
3	698	324	444	1259	2807	5014	7748
4	209	290	277	210	139	98	87
5	79.0	66.3	66.1	72.5	79.3	83.3	83.8
6	67.5	65.0	65.0	65.1	65.0	64.8	64.6
7	59.1	62.9	64.7	65.1	64.9	64.7	64.6
8	54.5	...	...	44.0	45.7	48.3	51.1
	Pauli form factor						
N	$b=1$	$b=1.5$	$b=2$	$b=2.5$	$b=3$	$b=3.5$	$b=4$
3	297	1089	2318	3762	5292	6853	...
4	166	111	56.0	38.1	78.3	183	...
5	14.1	25.6	35.1	37.4	34.6	30.0	...
6	13.2	13.8	15.1	17.6	19.8	21.7	...
7	12.8	13.0	13.3	...	14.6	15.4	...

TABLE IX. Coefficients for polynomial fits for different choices of b. The coefficients a_n and c_n and their diagonal errors for fits to the data of Table I using different values for the parameter b in Eq. (2).

	$b=1.5$		$b=2$		$b=2.5$		$b=3$		$b=3.5$	
n	a_n	Error	a_n	Error	a_n	Error	a_n	Error	a_n	Error
					Magnetic form factor, quintic fits:					
0	2.14	0.01	1.54	0.01	1.11	0.01	0.79	0.01	...	...
1	3.47	0.01	4.07	0.03	3.71	0.03	3.22	0.03	...	...
2	−2.35	0.02	5.29	0.07	2.08	0.04	2.99	0.04	...	...
3	−6.01	0.03	−4.59	0.22	−3.35	0.19	−2.20	0.17	...	...
4	1.07	0.07	−0.42	0.04	−1.33	0.04	−1.83	0.05	...	...
5	2.90	0.19	2.12	0.15	1.50	0.13	0.94	0.12	...	...
					Magnetic form factor, sextic fits:					
0	...	...	...	...	1.10	0.01	0.78	0.01	0.56	0.01
1	...	...	...	...	3.76	0.04	3.22	0.03	2.64	0.03
2	...	...	...	...	2.50	0.16	3.57	0.16	4.08	0.14
3	...	...	...	...	−3.72	0.23	−1.99	0.18	−0.23	0.26
4	...	...	...	...	−3.56	0.82	−4.63	0.74	−5.08	0.70
5	...	...	...	...	1.51	0.13	0.46	0.18	−0.63	0.26
6	...	...	...	...	1.51	0.55	1.97	0.52	2.22	0.52
					Pauli form factor, sextic fits:					
0	1.34	0.02	0.92	0.01	0.62	0.01	0.42	0.01	0.28	0.01
1	2.88	0.05	2.85	0.08	2.47	0.07	2.04	0.06	1.64	0.05
2	−1.56	0.36	0.98	0.10	2.11	0.11	2.61	0.15	2.77	0.19
3	−6.62	1.12	−4.20	0.63	−2.44	0.42	−1.12	0.31	−0.09	0.23
4	−1.92	0.64	−2.90	0.54	−3.08	0.50	−2.91	0.49	−2.54	0.50
5	3.39	0.66	1.95	0.36	0.97	0.24	0.27	0.17	0.28	0.13
6	1.80	0.53	1.61	0.28	1.35	0.30	1.07	0.28	0.77	0.27

We now examine the sensitivity of our results to the value of the parameter b used in Eq. (2), and we attempt to justify the choice $b=2$ used above. In I we introduced two criteria for the choice of b, and found they were both met for $b=2$. (i) The data for real η should be approximately centered around the origin. (For data used in I the centering suggests $b=2$; this criterion now suggests $b=3$ for the magnetic fit, since the range has been extended from -45 F^{-2} to -175 F^{-2}.) (ii) The peak in the spectral function should be near angle $\xi=90°$, since otherwise a fit with a truncated Fourier series tends to displace the peak towards 90°. This displacement effect was shown in I for artificial data based on a Clementel-Villi form factor. Equation (5) and Table V show that the peak near 700 MeV does indeed occur at $\xi=90°$ with the choice $b=2$.

In this paper we introduce two additional criteria for the choice of b. (iii) We examine in Table VIII the χ^2 values of the restricted fits versus both the value of b and the degree N of the polynomial. (iv) We examine in Table X the extrapolated value of $G(172)$ versus the value chosen for b.

The magnetic form factor value of $\chi^2=66.1$ for a quintic fit with $b=2$ is seen from Table VIII to be the lowest for any quintic fit. A sextic fit lowers the χ^2 so little that the slight improvement does not seem worthwhile, since the errors in the extrapolation increase rapidly with the degree of the polynomial. The improvement in χ^2 values for the octic fits is at the expense of such large errors that the extrapolated spectral function is worthless. The Pauli form factor has χ^2 values that are statistically acceptable for the whole range of b considered for either a quintic or a sextic fit. We choose the sextic fit. Thus the χ^2 argument suggests $b\approx 2$ for the conformal transformation for the magnetic form factor and does not argue against this value for the Pauli form factor fit. The coefficients a_n and c_n for different values of b are given in Table IX. We use these coefficients to find the value of G for annihilation into lepton pairs at $t=172$ F^{-2}, for different choices of b. For each b, we use the sextic fit to F_2. For $1.5\leq b\leq 3$ we use quintic fits to G_M, while for $2.5\leq b\leq 3.5$ we also use sextic fits to G_M. Table X shows that the values found for G are sensitive to the value chosen for b.

In the previous section we used this dependence of G on b to choose the value $b=2$ to obtain agreement with

TABLE X. Extrapolated value of G for annihilation. The total cross section for proton-antiproton annihilation into lepton pairs is proportional to G^2. We use the coefficients of Table IX to extrapolate the form factors to $t=172$ F^{-2} and use Eq. (12) to determine G; the statistical error given is only approximate.

b	G	Approximate error
	Quintic fit to magnetic form factor:	
1.5	1.2	0.1
2.0	2.5	0.1
2.5	3.9	0.2
3.0	5.0	0.3
	Sextic fit to magnetic form factor:	
2.5	1.4	0.4
3.0	2.6	0.7
3.5	5.2	1.3

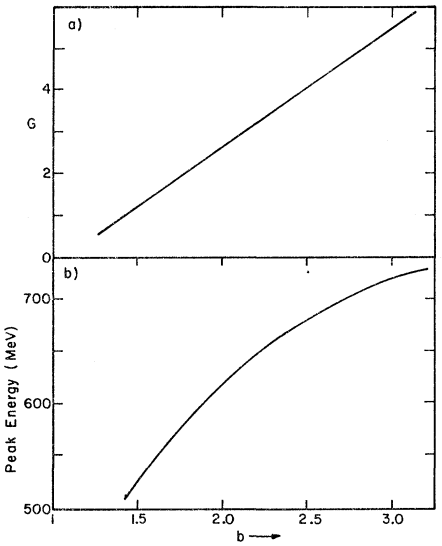

FIG. 6. Dependence of extrapolation on the value of the parameter b used in the conformal transformation (2). Plot (a) shows the dependence of G on b using Table X for quintic fits to the magnetic form factor. Plot (b) shows the position of the center of the peak in MeV for the magnetic spectral function, plotted versus the value of b.

the preliminary measurement of G. That is, the agreement found at the end of the previous section is *not* a fortuitous accident. However, it may be of significance that we are led to a value of b near 2 by three other arguments.

The choice of the value of b has only a modest effect on the magnetic spectral function near the main peak. Figure 6 compares the sensitivity of the value of G to our choice of b to the relative insensitivity of the energy of the peak of the magnetic spectral function. (In both cases we confine ourselves to quintic fits to the magnetic form factor.) When we vary b from 1.5 to 3, the value of G in Table X and Fig. 6(a) increases by a factor of 4; but the energy of the peak [Fig. 6(b)] varies only from 530 to 720 MeV. An accuracy of 25% in the measurement of G is sufficient to determine the value of b with sufficient accuracy for a 5% determination of the peak energy; note that this quoted 5% error in the peak energy is *only* that due to inaccuracies in knowledge of the value of b.

Of course, one can vary the degree N of the polynomial simultaneously with varying b, and Table X shows that in this case it is possible to keep the same value of G for a different value of b: cf. the quintic fit with $b=2$ and the sextic fit with $b=3$. One might wonder how much the magnetic spectral function would be affected by this simultaneous change in N and b. We compare the two spectral functions in Fig. 7. We find that the increase in the value of b does shift the peak energy to a higher value. The sextic fit with $b=3$ has a peak energy of 680 MeV, which we compare with 720 MeV for the quintic using $b=3$, and 620 MeV for the quintic using $b=2$. (The sextic fit is reproduced by Wilson and Levinger in their review paper.[4]) The error in the sextic fit is sufficiently large that there is not a clear disagreement between the two spectral functions of Fig. 7. Our picture of a peak around 625 MeV, a zero around 1050 MeV, and a dip around 1500 MeV remains unchanged.

In conclusion, we find that our extrapolated values of the proton's spectral functions are quite similar to those found in I, but that our confidence in the extrapolation procedure has increased. In particular, the main peak in the electric spectral function is not affected greatly by imposing the constraint that $G_E(4M^2)=G_M(4M^2)$, as illustrated in Fig. 4, though the dip around 1500 MeV is greatly changed. Further, as illustrated in Fig. 5, the magnetic spectral function is changed only a little by the use of an assumed datum at infinite momentum transfer. Finally, the value of the parameter b used in the conformal transformation (2) could be determined with sufficient accuracy by an inaccurate measurement of the annihilation cross section into lepton pairs.

However, there remains one important systematic error in our extrapolation procedure: namely, that if there really are a peak and a dip fairly close together, they are spread apart by our procedure of fitting with a truncated Fourier series. This effect is clearly shown by the artificial data illustrated in I, Fig. 11(b), where the input spectral function data consisted of 2 resonances located at 650 and 900 MeV. The artificial data were chosen to have a better accuracy than that of the real data used here; but the artificial data had a smaller range, and could be fitted with a quartic, as contrasted with the quintic fits here to the magnetic spectral function. The output spectral function successfully resolved the two peaks, but spread them apart to 550 and 1150 MeV, respectively. The position of the zero of the spectral function was not changed. If this system-

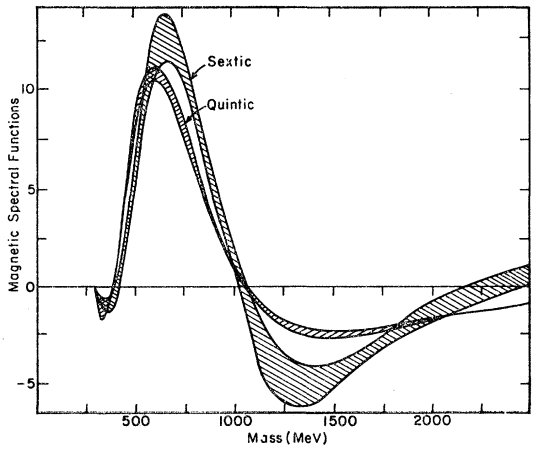

FIG. 7. Comparison of two magnetic spectral functions. The quintic using $b=2$ is taken from Table V; the sextic using $b=3$ has coefficients given in Table IX. The shaded regions show the statistical errors.

atic error is occurring to a similar extent in our present work, the magnetic spectral function peaks at 620 and 1400 MeV shown in Fig. 3 *might* actually represent the effects of a truncated Fourier series in fitting, say, a ρ-ω peak near 750 MeV, a ϕ at 1050 MeV, and a ρ' peak[5] at 1250 MeV. (Note that it is uncertain whether the ρ' is 1^-.) In any case, the region below 1000 MeV is not inconsistent with this interpretation. The position of the zero at 1050 MeV may well be more accurate than the positions of the peak or the dip. Finally, the value of G for the annihilation process argues for a long high energy tail on the spectral function, as in Fig. 3, rather than approximating the spectral function beyond 1000 MeV by a single pole.

ACKNOWLEDGMENTS

We are grateful to R. F. Peierls for the use of his computing program, and to the 1604 computer group for the actual computations. We wish to thank R. Hofstadter and K. W. Chen for sending us unpublished data on the proton form factors,[6] and to thank K. Barnes and F. Gross for discussions for the equality of electric and magnetic form factors at $t=4M^2$.

PHYSICAL REVIEW VOLUME 136, NUMBER 3B 9 NOVEMBER 1964

Possible Experimental Consequences of Triangle Singularities in Strange-Particle Production Processes*

Y. F. CHANG AND S. F. TUAN
Purdue University, Lafayette, Indiana
(Received 30 June 1964)

Observable consequences of anomalous threshold singularity for triangle diagrams are examined with special reference to cases where baryon resonances of narrow width participate as an internal line in the E channel. It is found that the reaction $K^-+p\rightarrow K+\pi+\Xi$, with Ξ^* (1530) included as an internal line of the graph, offers the best experimental situation for detecting an anomalous singularity effect by studying the $(K\pi)$ mass spectrum in final state.

I. INTRODUCTION

THE actuality of anomalous singularities has long been regarded by Goldberger as a critical test of present-day notions concerning the analyticity of transition amplitudes involving production reactions.[1] Indeed, in many of the dynamical approaches to strong-interaction physics, one abandons several important concepts in conventional field theory, yet, nevertheless, assumes that the singularities of the perturbation amplitude are maintained in the correct amplitude.[2] To the extent that one knows, on the strength of perturbation theory, that amplitudes for production reactions are in general characterized by the presence of various anomalous threshold singularities, both real and complex,[3–5] it is evidently of great importance to the current theoretical premise that experimental manifestations due to these singularities be found.

Landshoff and Treiman[1] first tackled this question in connection with simple triangle diagrams such as illustrated in Fig. 1, where E is the incoming energy, m and $\sqrt{s}$ are effective masses of particles emitting from the second and third vertices. The singularities we wish to observe are not poles, but provided they are infinites rather than simple branch points, there is hope that they can give rise to observable effects when they are close to the physical region. Landau[3] and Polkinghorne and Screaton[6] have prescribed rules that only the simplest graphs produce singularities of the infinity-type. Since the simple triangle diagrams are indeed the only graphs with three external vertices that give rise to infinities, they are the logical graphs to survey in the first instance.

The process considered by Landshoff and Treiman

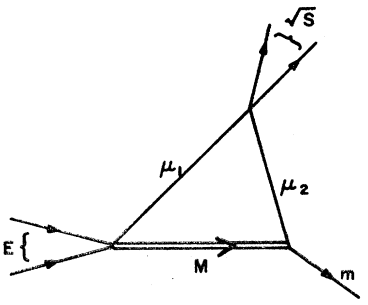

FIG. 1. Basic triangle graph under consideration.

* Work supported in part by the U. S. Air Force Office of Scientific Research and the National Science Foundation.

[1] P. V. Landshoff and S. B. Treiman, Phys. Rev. **127**, 649 (1962).

[2] H. P. Stapp, Phys. Rev. **125**, 2139 (1962); G. Källen and A. S. Wightman, Kgl. Danske Videnskab. Selskab, Mat. Fys. Medd. **1**, 6 (1958).

[3] L. D. Landau, Nucl. Phys. **13**, 181 (1959).

[4] R. E. Cutkosky, J. Math. Phys. **1**, 429 (1960).

[5] P. V. Landshoff and S. B. Treiman, Nuovo Cimento **19**, 1249 (1961).

[6] J. C. Polkinghorne and G. R. Screaton, Nuovo Cimento **15**, 925 (1960).